Molecular dynamics simulation of equilibrium configurations of plasmas containing multi-species dusts

2007 J. Phys. A: Math. Theor. 40 10383

(http://iopscience.iop.org/1751-8121/40/33/027)

IOP Publishing Journal of Physics A: Mathematical and Theoretical

J. Phys. A: Math. Theor. **40** (2007) 10383–10392 doi:10.1088/1751-8113/40/33/027

Molecular dynamics simulation of equilibrium configurations of plasmas containing multi-species dusts

Yanhong Liu and Lock Yue Chew

School of Physical and Mathematical Sciences, Nanyang Technological University, 637616 Singapore

Received 11 May 2007, in final form 4 July 2007
Published 1 August 2007
Online at stacks.iop.org/JPhysA/40/10383

Abstract

Equilibrium configurations of dusty plasmas with grains of different sizes, which interact through a screened Coulomb force field and confined by a two-dimensional quadratic potential, are studied using molecular dynamics simulation. The system configuration depends on the sizes, masses and charges of the grain species as well as the screening strength of the background plasma. The consideration of the grain size has established a different equilibrium configuration relative to that of point grains. In the new configurations, grains of different species separate into different shells, with the grains of larger mass and charge located away from the system center, forming a shell that surrounds the grains of smaller mass and charge at the system center. This configuration occurs beyond a critical grain radius, and its structure and size are determined by the competing effects between the inter-grain electrostatic repulsive force, the screening effect of the plasma and the mass-dependent confinement force of the quadratic potential.

PACS numbers: 61.50.Ah, 36.40.Wa, 61.43.Bn, 52.27.Lw

(Some figures in this article are in colour only in the electronic version)

1. Introduction

There has been growing interest in the studies of pattern formation through the process of particles self-assembly in different systems [1–9]. Examples of such systems are electrons confined in quantum dots [1], heavy ions in storage rings [2] and strongly coupled dusty plasmas [3, 4]. In most of these studies, only a single species of particles is considered. Recently, the properties of multi-species systems have begun to attract more attention [10–19]. For instance, Hornekær *et al* [10] have experimentally studied a two-component ionic crystal confined in a Paul trap and have found radial separation between the two ionic species.

Matthey *et al* [11] have numerically investigated a system containing two species of particles with an identical mass-to-charge ratio, and have observed a mixing of the two species which is independent of their relative abundances. Grzybowski *et al* [12, 13] have experimentally examined a two-dimensional (2D) system containing two ferromagnetic particles (disks) of different sizes located on a liquid-to-air interface in an external magnetic field. They found that depending on the experimental conditions, the particles can either separate or mix. Drocco and Nelissen *et al* [14–16] have studied a 2D binary system and have shown that in the ground state similar particles tend to group together, but mixing of the particles in the shells can appear if the mass and charge ratios of the corresponding species become equal. More recently, Liu *et al* [17] have studied the self-organized separation of multi-species dust grains by means of molecular dynamics (MD) simulation. They consider the dust grains interacting through a screened Coulomb potential with a long-range attractive component, in addition to being confined within a 2D quadratic trap. They have studied the effect of grain mass and charge on the organizational structure of multi-species dusty plasma.

In a dusty plasma, the grains interact with each other and give rise to dust molecule formation, agglomeration, dust cloud, as well as the formation of ordered structures such as the plasma crystals [20–25]. In fact, these ordered structures can serve as a platform for the investigation of condensed matter systems since the dust grains, being massive and large, enable the observation of macroscopic effects from microscopic events. For example, Khrapak *et al* [26, 27] experimentally investigated the compressional waves in a complex plasma under a microgravity condition. In the experiments, the two-species grains' separation is also observed. In an experimental investigation on a dusty plasma, the grain size can be large and comparable to the mean inter-grain distance. Hence, the consequence of the grain size on the system properties should not be neglected [28–31]. In fact, the effect of the grain size on the system structures of a 2D dusty plasma is still not clear [32]. Thus, it is of interest to study a 2D dusty plasma that contains grains of a different mass, charge and radius at different screening strengths in order to reveal the effects of the grain size and screening strength on the system properties.

This paper is organized as follows. In section 2, we present our model system and numerical approach. In section 3, we uncover the minimum-energy configurations of diverse two-species and three-species dusty plasmas with grains of a different mass, charge and radius. We discuss the principal effects of the grain radius and screening strength, as well as the grain mass and charge, on the equilibrium structure of the dusty plasma. In section 4, we present our conclusions.

2. Model system and numerical approach

We consider a 2D dusty plasma consisting of a finite number of grains of a different mass, charge and radius, interacting through a screened Coulomb force field [29–33], and confined by a quadratic potential [34, 35]. The Hamiltonian of the system is $H = K + U$, where K is the kinetic energy and

$$U = \sum_{i=1}^{N} \frac{1}{2} M_i \omega_0^2 r_i^2 + \frac{1}{\varepsilon} \sum_{i=1, i<j}^{N} \frac{Q_i Q_j}{(1 + a_i/\lambda)(1 + a_j/\lambda) r_{ij}} \mathrm{e}^{-(r_{ij} - a_i - a_j)/\lambda} \tag{1}$$

is the potential energy. In equation (1), $N = \sum_{s=1}^{n} N^{(s)}$ is the total grain number, with n being the total species number, and $N^{(s)}$ is the number of grains of species s. Note that M_i, Q_i, a_i and $\mathbf{r}_i$ are the mass, charge, radius and position of grain i $(=1, \ldots, N)$, respectively; $r_{ij} = |\mathbf{r}_i - \mathbf{r}_j|$; ω_0 is the trapping frequency of the external confinement potential; ε is the

dielectric constant of the surrounding medium and λ is the screening length. The potential energy given by equation (1) can also be written in the dimensionless form

$$U = \sum_{i=1}^{N} m_i r_i^2 + \sum_{i=1, i<j}^{N} \frac{q_i q_j}{(1+\kappa a_i)(1+\kappa a_j) r_{ij}} \mathrm{e}^{-\kappa(r_{ij}-a_i-a_j)}, \tag{2}$$

where the mass and charge have been normalized by the mass $M^{(1)}$ and charge $Q^{(1)}$ of grains of species 1 respectively, the space coordinate and energy have been normalized by $r_0 = \left(2Q^{(1)2}/M^{(1)}\varepsilon\omega_0^2\right)^{1/3}$ and $E_0 = M^{(1)}\omega_0^2 r_0^2/2$, respectively, and $\kappa = r_0/\lambda$ represents the strength of screening by the background plasma on the dust grains.

The existence of the separated layers corresponds to the balance of the vertical forces (such as the gravity, thermal and electrostatic sheath forces) acting on the grains. Existing investigations [36–41] showed that due to a self-organization process involving local-field, or space, dependent dust charging, the charge-to-mass ratio of the particles in each layer is usually the same. Since the system is slowly annealed to $T \sim 0$ in the simulation, isotropic (with respect to the particle) frictional forces such as neutral drag can be considered to be qualitatively included. Accordingly, we introduce the parameter $\mu^{(s)}$ $(=m^{(s)}/m^{(1)} = q^{(s)}/q^{(1)})$ to denote the grain mass or charge ratio that is kept constant in the layer. Since $m^{(1)} = 1$ and $q^{(1)} = 1$, $\mu^{(s)}$ $(s = 1, 2, \ldots, n)$ is simply the grain mass or charge of species s. According to [42] and [43], the charge on a dust grain is proportional to the radius of the grain. Hence, we have $a^{(s)} = \mu^{(s)} a^{(1)}$ $(s = 1, 2, \ldots, n)$. The species are distinguished by their different materials, or mass densities.

We use MD simulation to track the motion of the grains. To achieve the minimum-energy state $(H \to U)$, each run is started with a random spatial and velocity distribution of the grains that are set at a high temperature $(T = 0.05 \to 1.0$, where T has been normalized by $E_0)$. The system is then slowly annealed until the temperature reaches zero $(T = 0 \pm 10^{-6})$. The annealing time is $6 \times 10^4 \omega_0^{-1}$ and the integration time step is $0.003\omega_0^{-1}$. We have checked the accuracy of our simulations by comparing our results to the stable-state configurations of single or two-species clusters obtained from Monte Carlo or MD simulations [14, 15, 35]. Very good agreements were found.

3. Simulation results

In this section, we first study a dusty plasma with two species of grains by varying the grain radius $a^{(1)}$ and mass ratio (or charge ratio) $\mu^{(2)}$ at a fixed screening strength κ. We then investigate the same system, but now vary $a^{(1)}$ and κ while fixing $\mu^{(2)}$. We shall also study the effect of the grain radius and screening strength on fixed mass and charge ratios in a multi-species system. For each case, the minimum-energy system configurations are obtained and analyzed.

3.1. Systems with two species of grains

3.1.1. Different mass ratio or charge ratio. We first consider an $N = 100$ system containing two species of grains of a different radius and mass (charge) ratio, interacting through a screened Coulomb potential with a fixed screening strength of $\kappa = 4$. Figure 1 shows the minimum-energy configurations of this system. We have included the special case of $\mu^{(2)} = \mu^{(1)} = 1$ for comparison. The subfigures are arranged such that the columns show the effect of the grain mass ratio (or grain charge ratio) $\mu^{(2)}$, while the rows show the effect of the grain radius $a^{(1)}$ on the system structures. From figure 1, one observes that when

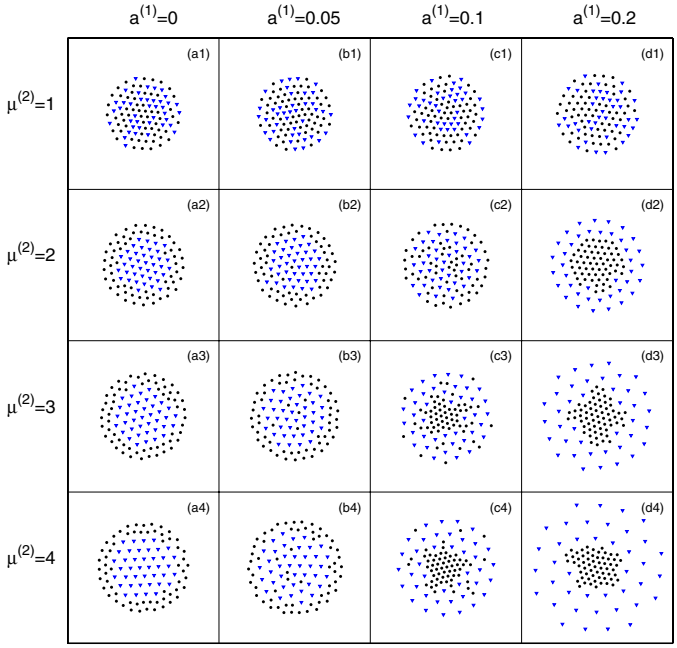

Figure 1. The minimum-energy configurations for two species of grains with a different radius, mass or charge ratio $\mu^{(2)}(=m^{(2)}/m^{(1)} = q^{(2)}/q^{(1)})$ at a fixed screening strength of $\kappa = 4$. The relation between the grain radii is $a^{(2)} = \mu^{(2)}a^{(1)}$. The total number of grains is $N = 100$, and the number of grains for species 1 (dots) and 2 (triangles) are $N^{(1)} = 60$ and $N^{(2)} = 40$ respectively. The subfigures are to the same arbitrary scale.

$\mu^{(2)} = \mu^{(1)} = 1$ (figures 1(a1), (b1), (c1) and (d1)), the grains are mixed together because the two species are physically indistinguishable. If we were to ignore the effect of the grain size by setting $a^{(1)} = 0$, the grains of species 2 are found to locate near to the system center, being surrounded by the grains of species 1 when $\mu^{(2)} \neq 1$. By turning on the grains radius through increasing $a^{(1)}$ (note that $a^{(2)} = \mu^{(2)}a^{(1)}$), the grains of species 2 begin to relocate outwards to the system edge, while the grains of species 1 gather inwards to the system center. At a critical value of $a^{(1)}$, the two species become completely separated, with species 2 forming a shell surrounding the grains of species 1. For example, at $\mu^{(2)} = 2$, the critical value is $a^{(1)} = 0.2$ (see figure 1(d2)). It is interesting to note that with larger $\mu^{(2)}$, the observed grain separation occurs at a smaller critical grain radius; at $\mu^{(2)} = 4$, the critical value reduces to $a^{(1)} = 0.1$ (see figure 1(c4)). Furthermore, we observe an increase in the system size when either $a^{(1)}$ or $\mu^{(2)}$ increases.

These results can be understood by first examining equation (2). In equation (2), the inter-grain potential can be viewed as the normal screened potential used for the case of point grains ($a^{(1)} = 0$) [25, 35] with a modified grain charge $q_{\rm mod} = q\,{\rm e}^{\kappa a}/(1 + \kappa a)$, where q and a are the grain charge and radius respectively [30]. The variation of the modified grain charge $q_{\rm mod}$ with grain radius a (at a fixed $\kappa = 4$) for different grain charge q is shown in figure 2. Figure 2 shows that the grain-modified charge increases with the grain radius. In addition, the figure shows a larger increase of modified grain charge with a for a larger grain charge q (for example, $q = 4$). Thus, for the two-species system with a fixed grain mass (charge) ratio $\mu^{(2)}$ (figure 1), increasing the grain radius $a^{(1)}$ increases the grain-modified charge

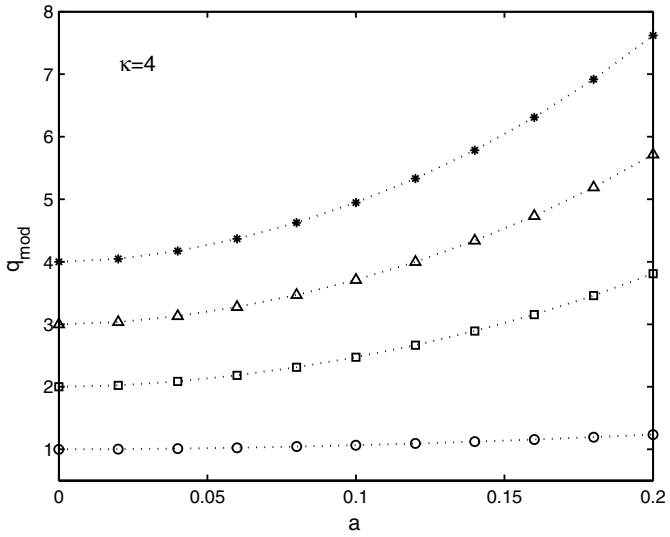

Figure 2. The variation of the grain-modified charge, $q_{\mathrm{mod}} = q\,\mathrm{e}^{\kappa a}/(1+\kappa a)$, with grain radius, a, at $\kappa = 4$ for different grain charges $q = 1$ (circle), 2 (square), 3 (triangle) and 4 (star).

$q_{\mathrm{mod}}^{(s)}$ ($s = 1$ and 2). This in turn increases the inter-grain repulsive force, resulting in a larger system size as observed in figure 1. For $\mu^{(2)} > 1$, an increase in $a^{(1)}$ leads to a much greater increase in the modified charge on grains of species 2 than that on species 1, and when the inter-grain repulsive force between species 2 becomes large enough, the grains begin to situate far apart from each other. Finally, at a critical value of $a^{(1)}$, they form a shell at the system edge surrounding the grains of species 1 as shown, for example, in figure 1(d2). At a larger $\mu^{(2)}$, the modified charge on grains of species 2 increases even faster with $a^{(1)}$. Hence, we expect the occurrence of grains separation at a smaller critical value of $a^{(1)}$. This is indeed illustrated in figure 1(c4) at $\mu^{(2)} = 4$ and $a^{(1)} = 0.1$. On the other hand, fixing $a^{(1)}$ (with $a^{(1)} > 0$) while increasing $\mu^{(2)}$ also leads to an increase in the modified charge on grains of species 2. Hence, we again expect grain separation at a critical value of $\mu^{(2)}$ as well as a corresponding increase in the system size. For the case of point grains with $a^{(1)} = 0$, the inter-grain repulsive force is short ranged and the inward mass-dependent confinement force becomes the dominant factor in determining the grains' position in the system. In this case, we expect the grains with the larger mass $\mu^{(2)}$ to be pushed near to the system center, being surrounded by a shell formed by the grains with the smaller mass $\mu^{(1)}$. The minimum-energy configuration for point grains is hence determined through the competition between the inward mass-dependent confinement force and the charge-dependent inter-grain repulsive force.

3.1.2. Different screening strengths. Next, we consider the same system but now fixing the grain mass (charge) ratio while varying the particle size and the screening strength κ. Figure 3 shows the minimum-energy configurations of the various cases with the grain mass (charge) ratio being fixed at $\mu^{(2)} = 2$. The subfigures are arranged such that the columns show the effect of the screening strength κ, while the rows show the effect of the grain radius on the system structures. From figure 3, one observes that for $\kappa = 3$, 5 or 7, the different grains separate into different shells at a certain critical radius $a^{(1)}$, with the grains of species 2 and 1 located in the outer and inner shells respectively. No grains' separation is observed, however,

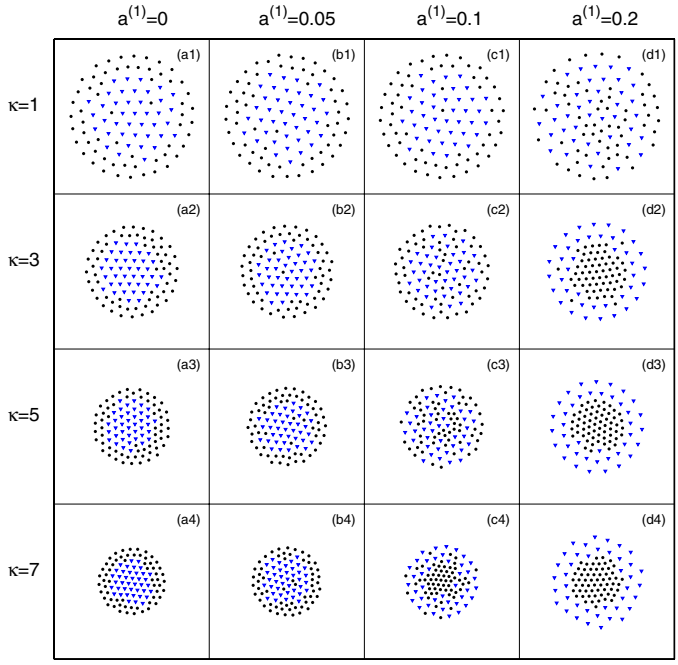

Figure 3. The minimum-energy configurations for two species of grains with different radius and screening strength κ at a fixed grain mass (charge) ratio of $\mu^{(2)} = 2$. The total number of grains is $N = 100$, and the numbers of grains for species 1 (dots) and 2 (triangles) are $N^{(1)} = 60$ and $N^{(2)} = 40$ respectively. The subfigures are to the same arbitrary scale.

for $\kappa = 1$. In addition, the grains' separation is observed to occur at a smaller critical radius for a higher κ, for example, at $a^{(1)} = 0.1$ when $\kappa = 7$ (see figure 3(c4)). If we were to fix $a^{(1)}$ and increase κ, one again observes particles' separation at a critical κ. However, for $a^{(1)} = 0$, the particles are separated in a different manner: species 2 at the system center, while species 1 form the surrounding shell. In all cases when $a^{(1)}$ is fixed, the whole system size is observed to decrease as κ increases.

This result can be understood with respect to the modified charge $q_{\rm mod}$ as before. Figure 4 shows the variation of the modified charge $q_{\rm mod}^{(1,2)}$ on grains of species 1 and 2 with $a^{(1)}$. The figure shows that at a fixed κ with $\mu^{(2)}(q^{(2)}) = 2, q_{\rm mod}^{(2)}$ increases much faster than $q_{\rm mod}^{(1)}$ as $a^{(1)}$ increases. In consequence, we expect a stronger inter-grain repulsive force between species 2, and at a critical value of $a^{(1)}$, the force becomes large enough to push the grains of species 2 far apart from each other, creating a shell at the system edge surrounding the grains of species 1. Furthermore, since $q_{\rm mod}^{(1,2)}$ increases much faster with $a^{(1)}$ at a larger κ (see figure 4), grains' separation is to be expected at a smaller critical radius at a higher κ, for example, $a^{(1)} = 0.1$ when $\kappa = 7$ as observed in figure 3(c4). On the other hand, grains' separation is not observed when $\kappa = 1$ because there is not much increase in the grain-modified charges as $a^{(1)}$ is increased from 0 to 0.2. This insignificant increase has also rendered the increase in the system size for $\kappa = 1$ to be unnoticeable, as opposed to the case of $\kappa = 3, 5$ and 7, where an increase in the whole system size with $a^{(1)}$ is obvious due to the more considerable rise in the modified charges on the grains. In addition to the modified charges, there is also the screening effect of the background plasma (represented by

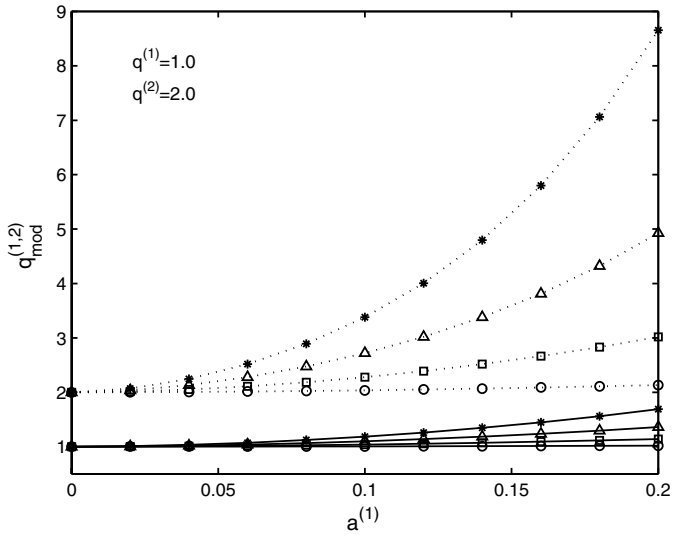

Figure 4. The variation of the grain-modified charge of species 1 (solid lines) and 2 (dotted lines) with the grain radius of species 1, at different screening strengths $\kappa = 1$ (circle), 2 (square), 3 (triangle) and 4 (star). Note that the grain charges of species 1 and 2 are fixed at $q^{(1)} = 1.0$ and $q^{(2)} = 2.0$ respectively.

$\exp(-\kappa r_{ij})$ in equation (2)), which serves to reduce the final inter-grain repulsive force as κ increases. Indeed, the final inter-grain repulsive force depends on the competing outcomes between the modified charges and the screening effects of the plasma. For example, by increasing κ at a fixed $a^{(1)}$, the screening effects can outweigh that due to the modified charges and lead to a decrease in the whole system size. This outcome is found to occur for $a^{(1)} = 0.05$ and $a^{(1)} = 0.1$. Conversely, at a larger $a^{(1)}$, for example $a^{(1)} = 0.2$, when these competing effects balance each other, the whole system size does not change much with increasing κ, as illustrated in figures 3(d2), (d3) and (d4) for $a^{(1)} = 0.2$. In the case of point grains, i.e. $a^{(1)} = 0$, the effect of the modified charges vanishes, and the system size reduces only due to plasma screening. In addition, the mass-dependent confinement force on the grains becomes important for point grains, leading to the minimum-energy configuration of the heavier species 2 at the system center, while species 1 forms a shell at the system edge.

3.2. Systems with three species of grains

Let us now consider an $N = 130$ system with three species of grains. We shall fix the grain mass (charge) of species 2 and 3 at $\mu^{(2)} = 2$ and $\mu^{(3)} = 3$, respectively, as we vary the grain radius of the different species and the screening strength of the dusty plasmas. Figure 5 shows the minimum-energy configurations of this system. From figure 5, one observes that at a fixed κ, the grains of species 3 move away from the system center as $a^{(1)}$ increases, while the grains of species 1 gather toward the system center. At $\kappa = 3$ and 5, grains' separation is found to occur at $a^{(1)} = 0.2$, with the grains of species 1, 2 and 3 being segregated into the inner, middle and outer shells respectively. In fact, for $\kappa = 5$, the trend of grains' separation already starts to appear at the smaller radius of $a^{(1)} = 0.1$. If we were to fix $a^{(1)} = 0$, the grains also show separation as κ increases, except that the grains of species 1, 2 and 3 now occupy the

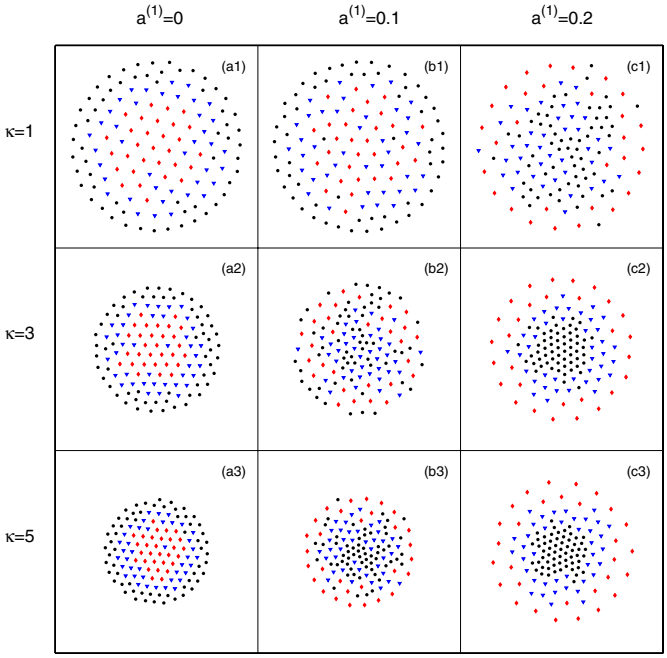

Figure 5. The minimum-energy configurations for three species of grains with different radius and screening strength κ at fixed grain mass (charge) ratios of $\mu^{(2)} = 2$ and $\mu^{(3)} = 3$. The total number of grains is $N = 130$, and the numbers of grains for species 1 (dots), 2 (triangles) and 3 (diamonds) are $N^{(1)} = 60$, $N^{(2)} = 40$ and $N^{(3)} = 30$ respectively. The subfigures are to the same arbitrary scale.

outer, middle and inner shells respectively. For a fixed $a^{(1)}$, in general, the whole system size is found to decrease as κ increases.

These results can again be understood as a consequence of the competition between the inter-grain repulsive force, the plasma screening effect and the confinement force of the quadratic potential. For example, since $q^{(3)}_{\rm mod}$ increases much faster than $q^{(2)}_{\rm mod}$ or $q^{(1)}_{\rm mod}$ with $a^{(1)}$, the greater inter-grain repulsive force between grains of species 3 pushes the grains further away from each other, establishing a shell around the grains of species 1 and 2 beyond the critical radius. Similarly, because $q^{(2)}_{\rm mod}$ increases faster than $q^{(1)}_{\rm mod}$ with $a^{(1)}$, we also expect grains of species 2 to surround species 1 above a certain critical grain size. As a result, we observe grains' separation, with the grains of species 1, 2 and 3 segregated into the central region, the middle shell and the outer shell respectively, as shown in figure 5(c3) at $\kappa = 5$ and $a^{(1)} = 0.2$. On the other hand, when $a^{(1)} = 0$, the dominating effects of the inward mass-dependent confinement force lead to the heavier grains of species 3 to accumulate at the system center, being successively surrounded by the lighter species 2 first, and then by the lightest species 1. Analogous to section 3.1.2, the whole system size tends to decrease as κ increases at a fixed $a^{(1)}$. However, when the grain size becomes sufficiently large, the competing effect of the increased modified charge balances the screening effect, negating the shrinking of the overall system size (see figures 5(c2) and (c3)).

We have also investigated much larger and complicated systems (not shown) with more grains and species. The results confirm the grain-separation behavior discussed here. This

shows the importance of the grain size or composition, as well as the effect of plasma screening on the equilibrium structures of a dusty plasma.

4. Conclusions

In conclusion, the above discussion shows that the grain size has an important bearing on the equilibrium configurations of a multi-species dusty plasma. The original equilibrium configuration of point grains, with grains of larger mass at the system center and grains of smaller mass at the system peripheral, is no longer a stable configuration with the consideration of the grain size. In fact, as the grain size increases, the grains with the larger mass relocate themselves at the system edges, forming a shell around the grains of smaller mass, which now reorganize themselves within the system center.

In a single-species system, the effects of the grain mass, charge and radius on the final system structures at various screening strengths may be envisaged, but their effects within a multi-species system are not evident. In this respect, the results here should provide insight into the equilibrium properties of multi-species systems. If a specific configuration of a multi-species dusty plasma is observed experimentally, our results can be useful for estimating the screening strength of the plasma and perhaps also to understand the grain growth (size change). Our results can be useful in guiding future investigations on the effects of the grain charge, mass and size on the equilibrium configurations and their wave behavior [26, 27] of multi-species dusty plasmas.

Acknowledgments

The authors thank Dr M Y Yu and Dr Z Y Chen for many helpful discussions.

References

[1] Ashoori R C 1996 *Nature* **379** 413
[2] Hangst J S, Nielsen J S, Poulsen O, Shi P and Schiffer J P 1995 *Phys. Rev. Lett.* **74** 4432
[3] Chu J H and Lin I 1994 *Phys. Rev. Lett.* **72** 4009
[4] Liu Y H, Liu B, Yang S Z and Wang L 2002 *J. Phys. A: Math. Gen.* **35** 9535
[5] Grimes C C and Adams G 1979 *Phys. Rev. Lett.* **42** 795
[6] Totsuji H, Kishimoto T and Totsuji C 1997 *Phys. Rev. Lett.* **78** 3113
[7] Bedanov V M and Peeters F M 1994 *Phys. Rev.* B **49** 2667
[8] Kong M, Vagov A, Partoens B, Peeters F M, Ferreira W P and Farias G A 2004 *Phys. Rev.* E **70** 051807
[9] Schweigert V A and Peeters F M 1995 *Phys. Rev.* B **51** 7700
[10] Hornekær L, Kjærgaard N, Thommesen A M and Drewsen M 2001 *Phys. Rev. Lett.* **86** 1994
[11] Matthey T, Hansen J P and Drewsen M 2003 *Phys. Rev. Lett.* **91** 165001
[12] Grzybowski B A, Jiang X, Stone H A and Whitesides G M 2001 *Phys. Rev.* E **64** 011603
[13] Grzybowski B A, Stone H A and Whitesides G M 2000 *Nature* **405** 1033
[14] Drocco J A, Reichhardt C J O, Reichhardt C and Jankó B 2003 *Phys. Rev.* E **68** 060401
[15] Ferreira W P, Munarin F F, Nelissen K, Filho R N C, Peeters F M and Farias G A 2005 *Phys. Rev.* E **72** 021406
[16] Nelissen K, Partoens B and Peeters F M 2004 *Phys. Rev.* E **69** 046605
[17] Liu Y H, Chen Z Y, Yu M Y and Bogaerts A 2006 *Phys. Rev.* E **74** 056401
[18] Liu Y H, Chen Z Y, Huang F, Yu M Y, Wang L and Bogaerts A 2006 *Phys. Plasmas* **13** 052110
[19] Ostendorf A, Zhang C B, Wilson M A, Offenberg D, Roth B and Schiller S 2006 *Phys. Rev. Lett.* **97** 243005
[20] Melzer A, Homann A and Piel A 1996 *Phys. Rev.* E **53** 2757
[21] Thomas H, Morfill G E, Demmel V, Goree J, Feuerbacher B and Möhlmann D 1994 *Phys. Rev. Lett.* **73** 652
[22] Melzer A, Nunomura S, Samsonov D and Goree J 2000 *Phys. Rev.* E **62** 4162
[23] Liu B and Goree J 2005 *Phys. Rev. Lett.* **94** 185002
[24] Pieper J B, Goree J and Quinn R A 1996 *Phys. Rev.* E **54** 5636

[25] Liu B and Goree J 2007 *Phys. Rev.* E **75** 016405
[26] Khrapak S *et al* 2003 *Phys. Plasmas* **10** 1
[27] Kretschmer M, Khrapak S A, Zhdanov S K, Thomas H M, Morfill G E, Fortov V E, Lipaev A M, Molotkov V I, Ivanov A I and Turin M V 2005 *Phys. Rev.* E **71** 056401
[28] Agarwal A K and Prasad G 2005 *Phys. Lett.* A **341** 479
[29] Hwang H H and Kushner M J 1997 *J. Appl. Phys.* **82** 2106
[30] Resendes D P 1998 *Phys. Scr.* T **75** 244
[31] Vyas V, Hebner G A and Kushner M J 2002 *J. Appl. Phys.* **92** 6451
[32] Fortov V E, Ivlev A V, Khrapak S A, Khrapak A G and Morfill G E 2005 *Phys. Rep.* **421** 1
[33] Resendes D P, Shukla P K and Morfill G E 2000 *Phys. Scr.* **62** 491
[34] Ezaki T, Mori N and Hamaguchi C 1997 *Phys. Rev.* B **56** 6428
[35] Cândido L, Rino J, Studart N and Peeters F M 1998 *J. Phys.: Condens. Matter* **10** 11627
[36] Ma J X, Liu J Y and Yu M Y 1997 *Phys. Rev.* E **55** 4627
[37] Denysenko I, Yu M Y, Ostrikovb K, Azarenkov N A and Stenflo L 2004 *Phys. Plasmas* **11** 4959
[38] Denysenko I, Yu M Y, Stenflo L and Azarenkov N A 2005 *Phys. Plasmas* **12** 042102
[39] Denysenko I, Ostrikov K, Yu M Y and Azarenkov N A 2006 *Phys. Rev.* E **74** 036402
[40] Vrancken R, Paeva G V, Kroesen G M W and Stoffels W W 2005 *Plasma Sources Sci. Technol.* **14** 509
[41] Liu B, Avinash K and Goree J 2004 *Phys. Rev.* E **69** 036410
[42] Samsonov D and Goree J 1999 *Phys. Rev.* E **59** 1047
[43] Chu J H, Du J B and Lin I 1994 *J. Phys. D: Appl. Phys.* **27** 296